

Stephan Holz^{1,*}
 Peter Köster¹
 Holger Thielert²
 Zion Guetta²
 Jens-Uwe Repke¹


Investigation of the Degradation of Chelate Complexes in Liquid Redox Desulfurization Processes

Metal complexes such as Fe-EDTA, which are used as pseudo-catalysts or oxygen carriers in wet oxidative desulfurization processes, are subject to a degradation mechanism that significantly influences the economics of such processes. Therefore, this study presents a methodology for determining the degree of degradation during the reactive hydrogen sulfide absorption in a Fe-EDTA solution within a continuously operating semi-batch reactor system. For this purpose, the reactive conversion of H₂S in the liquid phase was used as a reference, and a clear dependence of the degradation on the pH could be shown. In addition, indicators are introduced that evaluate the observed pH dependency of the degradation and distinguish pH-induced effects such as the pH-dependent absorption performance of H₂S.

Keywords: Chelate degradation, Ethylenedinitrilotetraacetic acid (EDTA), H₂S oxidation, H₂S removal, Liquid redox

Received: July 30, 2019; *revised:* October 8, 2019; *accepted:* December 17, 2019

DOI: 10.1002/ceat.201900420

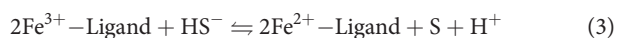
 This is an open access article under the terms of the Creative Commons Attribution License, which permits use, distribution and reproduction in any medium, provided the original work is properly cited.

1 Introduction

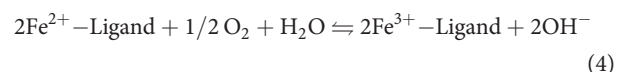
Wet oxidative desulfurization processes have been used since the beginning of the 20th century for the removal of H₂S from various process gases. The processes operate on the principle of absorption and oxidation of hydrogen sulfide to elemental sulfur by using an iron chelate or a quinone compound as pseudo-catalyst that can be regenerated with air [1]. Wet oxidative processes replace so-called dry oxidative processes such as the iron oxide process, since they are comparatively inefficient and characterized by high operating costs, high space requirements, and by poor quality of the recovered sulfur.

Compared with so-called neutralization processes, which operate on the principle of absorption and desorption, wet oxidative processes have the advantage that they can selectively separate H₂S and form sulfur directly due to the reaction mechanism with an iron chelate complex, as shown in Eqs. (1)–(4).

Absorption and sulfur formation:



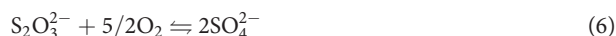
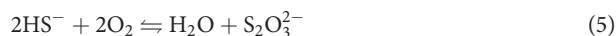
Regeneration:



Usually, the cycle described above consists of absorption and regeneration and takes place in two separate reaction zones, as shown in Fig. 1. Hydrogen sulfide is converted to sulfur in the column in an oxygen-lean atmosphere. Then, the sulfur is separated, and the reduced pseudo-catalyst is regenerated with air in the oxidizer or so-called regenerator.

If H₂S is not already converted into elementary sulfur by the pseudo-catalyst in the absorption column, the hydrogen sulfide anions are oxidized via thiosulfate to sulfate by the oxygen that is required for the pseudo-catalyst regeneration or when the lean solution fed to the absorber contains a large amount of dissolved oxygen [1]. Eqs. (5) and (6) therefore show the by-product formation.

By-product formation:



The pH value is one of the major operation parameters and must be maintained at the optimal level. If the pH value of the

¹Stephan Holz, Peter Köster, Prof. Dr.-Ing. habil. Jens-Uwe Repke
 stephan-holz@gmx.net

Technische Universität Berlin, Chair of Process Dynamics and Operations, Strasse des 17. Juni 135, 10623 Berlin, Germany.

²Dr.-Ing. Holger Thielert, Dr.-Ing. Zion Guetta
 thyssenkrupp Industrial Solutions AG, Friedrich-Uhde-Strasse 15,
 44141 Dortmund, Germany.

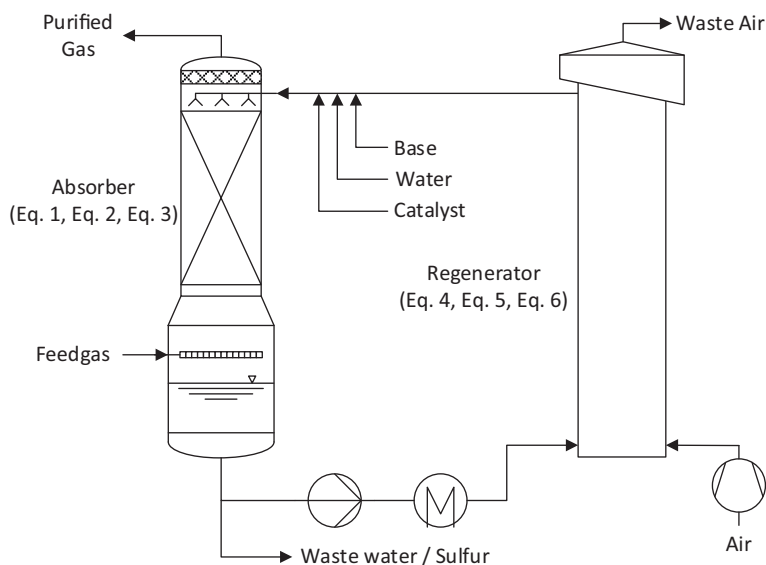


Figure 1. Flow sheet of a typical liquid redox process.

solution can drift above its normal working range of pH 8–8.5, the oxygen content of the solution will rise and thiosulfate formation will increase, as the solubility of oxygen increases with the pH value.

If the pH value is too low, H₂S absorption and reaction are adversely affected. The formation of thiosulfate and sulfate ions tends to reduce the pH value of the scrubbing solution and, consequently, the H₂S removal efficiency [1].

A disadvantage of iron chelate-based processes lies in the degradation of the pseudo-catalyst. The development of a suitable method and the investigation of the influence of the pH value on the degree of degradation under constant conditions are therefore the aims of the investigations presented in this study.

2 State of Knowledge

McManus and Martell [2] show that thiosulfate as a by-product acts as a radical scavenger and thus as an antioxidant, thereby reducing the degradation rate by up to one order of magnitude and thus significantly extending the stability of the pseudo-catalyst. The authors also postulate the following factors that influence the cost-effectiveness of chelate-based desulfurization processes:

- The degradation rate of the chelate complex depends on the type of ligand used.
- The solubility of the chelate complex depends on the type of ligand used.
- The reaction rate of the chelate complex in absorption and regeneration depends on the type of ligand used.

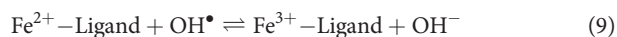
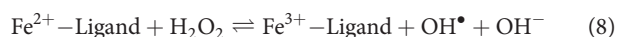
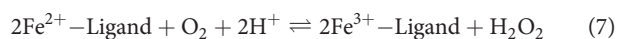
Saelee and Bunyakan [3] investigate the kinetics of degradation of iron ethylenedinitrilotetraacetic acid (Fe-EDTA) depending on the stabilizers sodium citrate and sodium thiosulfate, the H₂S feed concentration, and the initial Fe(III)-EDTA concentration within the wash solution. They come to the conclusion that the degradation follows a pseudo-first-order reac-

tion with respect to iron and develop a correlation for the degradation rate of Fe(III)-EDTA, but they also note that in each of their experiments the pH value has not been kept constant and decreases from pH 7 to 4.5.

Deshmukh and Shete [4] also investigate the degradation kinetics of the ligands nitrilotriacetic acid (NTA), EDTA, and diethylenetriaminepentaacetic acid (DTPA) in a semi-batch reactor at an initial pH value of approximately 6.0. In their test description, they only mention that the pH value has been measured over the test duration and not that it is continuously stabilized to a fixed value.

McManus and Martell [2] state in the description of their experiments for their iron chelate degradation studies that the pH value is not fixed and is only kept between pH 7 and 8.

Kohl and Nielsen [1] attribute the degradation mechanism to the formation of hydroxyl radicals and state the overall reaction mechanism as in Eqs. (7)–(10). Due to the degradation of the chelate complex, the ligand is no longer able to hold iron in solution. The dissolved iron then reacts to insoluble iron compounds and loses the ability to oxidize and reduce the hydrogen sulfide.



Wubs and Beenackers [5] have investigated the reaction rate of hydrogen sulfide with iron chelates and have found out that the pH value has a significant influence on the reactive H₂S absorption in solutions of chelated iron. Therefore, they continuously control the pH value in their experimental studies by the addition of basic additives over the entire duration of their experiments ($t_{\text{exp}} < 350 \text{ s}$)¹⁾ in order to be able to minimize the pH value-dependent effects as far as possible. However, due to the short duration of the experiment and the way it was carried out, no degradation effects were found.

In summary, it can be stated that the absorption of H₂S into a solution containing iron chelate depends on the pH value, which suggests that the degradation depends on the pH value as well. Due to the fact that, in the previous investigations on the degradation of iron chelate complexes, no constant conditions were created that reveal the influences induced by the pH value, in this contribution a systematic experimental investigation is presented that allows determining the degree of degradation under constant conditions.

1) List of symbols at the end of the paper.

3 Materials and Methods

3.1 Experimental Setup and Materials

The experiments were carried out as shown in Fig. 2 in a stirred glass reactor with a total volume of 1000 mL in semi-batch mode, in which approximately 700 mL redox solution was added. The test rig was operated with Linde test gas with 1500 ppmv ($\pm 2\%$) H_2S on N_2 basis. The feed gas flow was adjusted with a mass flow controller (MFC) and introduced into the redox solution via an immersion tube. The air flow for the regeneration of the pseudo-catalyst was also controlled via an MFC and distributed via a glass drip in the redox solution for better dispersion. The H_2S , O_2 and SO_2 concentrations in the flue gas were quantified with a Testo 350 analysis box. The pH value was measured by a measuring probe with local transmitter (Ingold pH 64) and recorded like the feed flows of H_2S and air by a process control system from ABB Ltd.

The pH value was adjusted by adding the basic additive (NH_3 solution; Merck EMPLURA 32 Ma. %) by means of a syringe-dosing pump (Chemyx Fusion 100 infusion pump) in order to keep the pH value constant throughout the complete duration of the experiments. Samples could be taken from the liquid phase at any time via a cannula with a closure valve inserted through a septum. The $\text{H}_2\text{S}(\text{aq})$ of the liquid phase was quantitatively investigated by silver nitrate precipitation in an automatic titrator (Metrohm 736 GP Titrimo).

3.2 Experimental Procedure

The Fe-EDTA solution was made of EDTA-chelated iron from the company dephyte e.K., which indicates an iron content of 13.3%. Therefore, an aqueous Fe-EDTA solution of 700 mL completely desalinated water with $\sim 4.0 \times 10^{-4}$ wt % Fe was prepared as redox solution. As basic additive, a 10-wt % NH_3 solution was added to the syringe, which was used to adjust the pH value. During the experiment, the pH value was kept constant by adjusting the dosing rate of the NH_3 solution. The air flow was adjusted to $\dot{V}_{n,\text{air}} = 4 \text{ L min}^{-1}$ after the stirrer speed of 1200 rpm was set. Afterwards the NH_3 dosage was switched on to be able

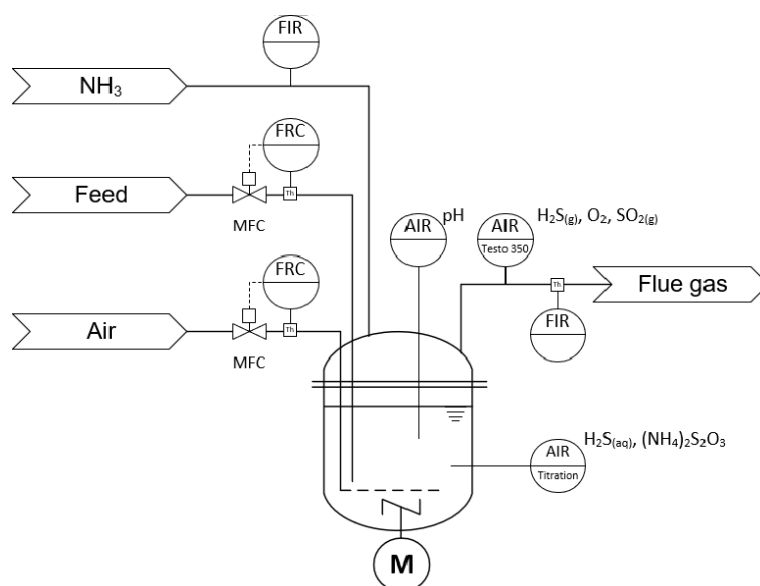


Figure 2. Experimental setup (semi-batch system).

to adjust the pH value to a constant value. After the pH value was constant, the feed gas $y_{\text{H}_2\text{S},\text{feed}} = 1500 \pm 2\%$ ppmv was adjusted to $\dot{V}_{n,\text{feed}} = 1 \text{ L min}^{-1}$ simultaneously with the airflow over the entire duration of the experiment. Due to the stoichiometric excess and the fine distribution of the air with the help of the glass drip, 100% regeneration of the pseudo-catalyst could be guaranteed at any time. During the experiments, analyses of the exhaust gas ($y_{\text{H}_2\text{S},(\text{g})}$, $y_{\text{O}_2,(\text{g})}$, $y_{\text{SO}_2,(\text{g})}$) and the redox solution ($x_{\text{H}_2\text{S},(\text{aq})}$) were carried out at regular intervals. The liquid phase was analyzed by titration by double determination. Due to the low concentration and the high load of H_2S , degradation of the ligand within 10 h was possible.

Three pH value levels (7.5, 8.5, 9.5) were investigated at ambient pressure and temperature, whereby pH 8.5 lies within the usual operating range of wet oxidative processes [6]. The respective experiments were repeated twice to ensure reproducibility and they could be reliably reproduced. The experimental pairs V1, V2 and V3, V4 and V5, V6 were performed with the exact operating conditions. Apart from the pH value, the same operating conditions were chosen for all experiments, V1 to V6, in order to guarantee comparability. Tab. 1 shows an overview of the operation conditions of all the experiments carried out.

Table 1. Operation conditions of the degradation experiments.

Experiment	pH [-]	$\dot{V}_{n,\text{feed}}$ [L min ⁻¹]	$y_{\text{H}_2\text{S},\text{feed}}$ [ppmv]	$\dot{V}_{n,\text{air}}$ [L min ⁻¹]	ξ_{Fe} [-]	ξ_{NH_3} [-]	T [K]	p [bar]	t_{exp} [h]
V1	7.5	1.0	1500	4.0	4×10^{-6}	0.1	ambient	ambient	10
V2									9
V3	8.5	1.0	1500	4.0	4×10^{-6}	0.1	ambient	ambient	9
V4									9
V5	9.5	1.0	1500	4.0	4×10^{-6}	0.1	ambient	ambient	9
V6									9

4 Results and Discussion

The evaluation includes the methodological approach to evaluate the degradation of the chelate complex Fe-EDTA. For this purpose, a degree of degradation was introduced. Based on further introduced key figures, a comparative analysis of the degradation experiments was carried out, in order to be able to quantify different effects.

4.1 Degree of Degradation

Fig. 3 shows an example of the trends of the exhaust gas concentration $H_2S(g)$ and the concentration of dissolved $H_2S(aq)$ for experiment V3 at the pH value 8.5. The corresponding trends of the ammonia dosing and the pH value are shown in Fig. 4. During all experiments, no SO_2 could be detected.

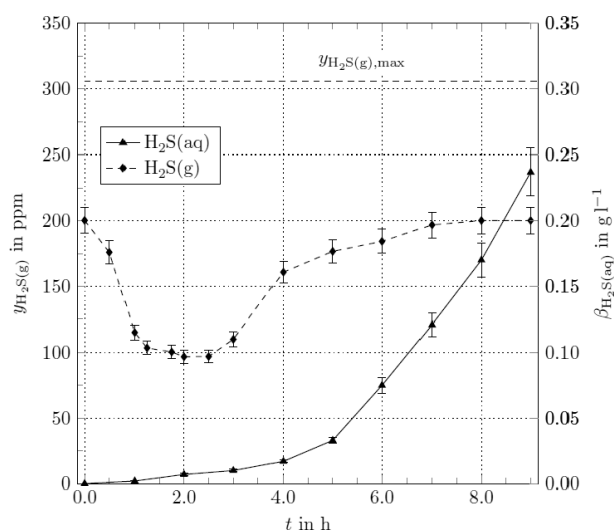


Figure 3. The trend of the H_2S concentrations for experiment V3.

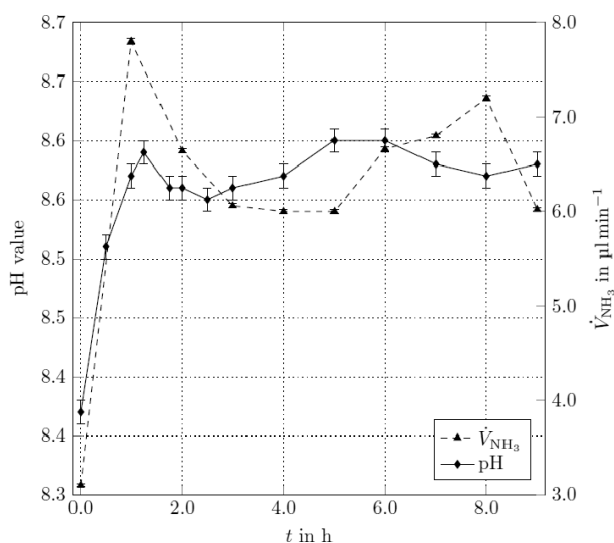


Figure 4. The trends of the pH value and the NH_3 dosage for experiment V3.

In principle, the behavior is the same for all investigated pH values. The exhaust gas concentration $H_2S(g)$ initially falls to a minimum value and then rises again steadily. The concentration of dissolved $H_2S(aq)$ increases slowly at first, then more and more rapidly. The curve shape of both concentrations can be explained by the increasing degradation of the ligand. By the degradation of the ligand, iron becomes free and then forms iron sulfide (FeS) together with the already formed sulfur. In this study, the iron sulfide was not quantified.

If iron is present in form of the ions Fe^{2+} or Fe^{3+} , the absorption of H_2S from the gas phase is controlled by the superimposed redox cycle according to Eqs. (3) and (4), which represents a sink for H_2S in the liquid phase. If iron is bound in the form of FeS , the redox cycle can no longer be completed. The absorbed $H_2S(aq)$ no longer reacts and $H_2S(aq)$ accumulates in the liquid phase until saturation is reached. The accumulation in the liquid phase increases with the progressive rate of the degradation, and the reactive absorption increasingly changes into a pure absorption with NH_3 buffering. The driving concentration difference between the gas and liquid phases becomes smaller and the $H_2S(g)$ in the exhaust gas increases. When the liquid phase is completely saturated with $H_2S(aq)$, no further $H_2S(g)$ can be absorbed from the gas phase and the concentration reaches the maximum value of $H_2S(g)$, which results from the pure mixture of $\dot{V}_{n,feed}$ and $\dot{V}_{n,air}$.

The initial decrease of the concentration of $H_2S(g)$ in the exhaust gas is due to the readjustment of the pH value after the addition of the feed gas.

For a comparison of the experiments, it is necessary to quantify the progressing degradation, and therefore the degree of degradation DD is introduced. The degree of degradation can be calculated by the ratio of the amount of substance of $Fe^{2+/3+}$ precipitated at time t to the amount of substance of $Fe^{2+/3+}$ initially used at time t_0 .

However, it is very difficult to measure the concentrations of Fe^{2+} and Fe^{3+} at certain points in time. The reason lies in the time lag between sampling and analysis, because all reactants for the redox cycle and for the radical mechanism are present in dissolved form within the liquid sample and both mechanisms take place simultaneously. In addition, the concentration of the redox catalyst is very low so that the result would be falsified by the advancing reactions.

For this reason, the degree of degradation is calculated in a different way. It is assumed that the conversion of $H_2S(aq)$ to the products only takes place at a sufficiently fast rate due to the redox catalyst $Fe^{2+/3+}$ and that the conversion without catalyst can be neglected [7]. This is because the reacting mass flow of $H_2S(aq)$ at any time is directly proportional to the mass flow of the remaining amount of $Fe^{2+/3+}$ ions. The assumption is justified to the effect that an oxidation of hydrogen sulfide to sulfur dioxide, like in the Claus process, can be excluded under the given operating conditions and the short residence time within the reactor. Furthermore, no sulfur dioxide could be detected in the exhaust gas during the experiments and the kinetics of sulfur formation with Fe-EDTA [8] is, in comparison to those of the by-products thiosulfate or sulfate, almost instantaneous.

With increasing degradation, the reactivity of the redox solution decreases, which can be used as a measure for calculating

the degree of degradation (DD). Eq. (11) defines DD as the decrease of the reaction rate to a reduced value at time t related to the maximum reaction rate of the redox solution. Therefore, it is a measure of how much of the active redox couple within an experiment has been converted into its inactive form. The maximum degree of degradation is 1 and illustrates the complete degradation of the Fe-EDTA. In this case, no further H_2S can react in the liquid phase to elemental sulfur according to Eq. (3).

The discrete determination of the rate of H_2S reaction, $\dot{n}_{H_2S, \text{reac}}(t)$, by liquid analysis makes it difficult to identify the maximum rate of reaction over time. Nevertheless, the results show that a maximum DD of 1 can be achieved, whereby a systematic error can be excluded.

$$DD(t) = 1 - \frac{\dot{n}_{H_2S, \text{reac}}(t)}{\dot{n}_{H_2S, \text{reac}, \text{max}}} \quad (11)$$

Since the degradation and the associated formation of the sparingly soluble FeS are irreversible, the quantity flow of the reacting $H_2S(aq)$ decreases continuously and is therefore highest at the beginning of the experiment when no degradation has occurred.

The reaction rate at certain points in time is calculated by a component balance for H_2S around the liquid phase and results according to Eq. (12) from the difference between the absorbed and stored $H_2S(aq)$ rates.

$$\dot{n}_{H_2S, \text{reac}}(t) = \dot{n}_{H_2S, \text{abs}}(t) - \frac{dN_{H_2S(aq)}}{dt} \quad (12)$$

The instantaneous molar flux, $\dot{n}_{H_2S, \text{reac}}(t)$, can be calculated with a component balance for H_2S around the gas phase according to Eq. (12), wherein the total exhaust gas flow is calculated as the sum of the feed and the air flow.

$$\dot{n}_{H_2S, \text{abs}} = (y_{H_2S, \text{feed}} \dot{V}_{n, \text{feed}} - y_{H_2S} (\dot{V}_{n, \text{feed}} + \dot{V}_{n, \text{air}})) \frac{P_n}{RT_n} \quad (13)$$

The capacity term $dN_{H_2S(aq)} dt^{-1}$ in Eq. (14) is estimated by using the measured $H_2S(aq)$ concentrations and a linear averaging between the discrete points of liquid sampling in time.

$$\begin{aligned} \frac{dN_{H_2S(aq)}}{dt} &\approx 0.5 \frac{N_{H_2S(aq)}(t_k) - N_{H_2S(aq)}(t_{k-1})}{t_k - t_{k-1}} \\ &+ 0.5 \frac{N_{H_2S(aq)}(t_{k+1}) - N_{H_2S(aq)}(t_k)}{t_{k+1} - t_k} \end{aligned} \quad (14)$$

Exemplarily, the calculated reaction power and the resulting degree of degradation for a pH value of 8.57 are shown in Fig. 5, with linear approximation between the discrete measuring points t_k .

Fig. 5 confirms the assumption of a continuously progressing and irreversible degradation and shows that the error increases with increasing test dura-

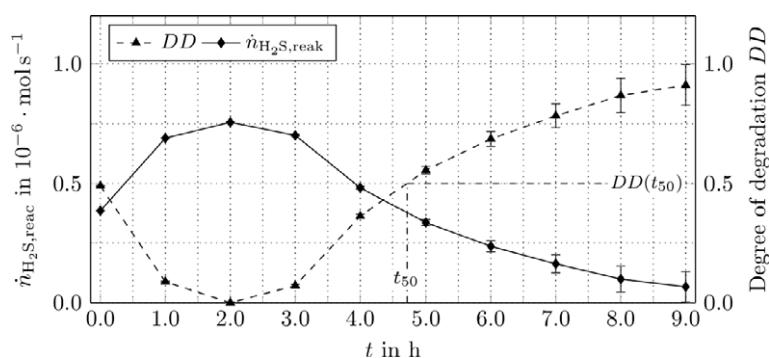


Figure 5. Degree of degradation DD and H_2S molar flux over time of experiment V3 (averaged pH value of experiment V3 = 8.57).

tion. The error increase results from the increasing $H_2S(aq)$ concentration and the associated increasing error due to the titration.

Fig. 6 shows the characteristics of the degree of degradation over the test period for all experiments performed. The degradation for higher pH values starts earlier and proceeds faster. However, the maximum degree of degradation is not achieved within the experimental period. This is largely due to the calculation methodology of the degree of degradation and the low concentrations and the associated measurement inaccuracy. Within the measurement uncertainty, an approximation to the maximum value can be determined.

In order to be able to make a statement about the stability of Fe-EDTA at varying pH values, a temporal comparison of the degree of degradation is not sufficient. Several effects occur that are dependent on the pH value. On the one hand, the absorption capacity of $H_2S(g)$ increases with increasing pH value, which leads to a higher H_2S stress of the redox catalyst or pseudo-catalyst in the liquid. On the other hand, due to the buffering effect of free NH_3 , $H_2S(g)$ separation from the gas stream is achieved even when the redox catalyst is already subjected to degradation and the absorbed $H_2S(aq)$ can no longer react.

The following section therefore introduces several indicators that consider these effects and show the effect of the pH value on the stability of the redox catalyst. The method presented can be applied to other pseudo-catalysts as well.

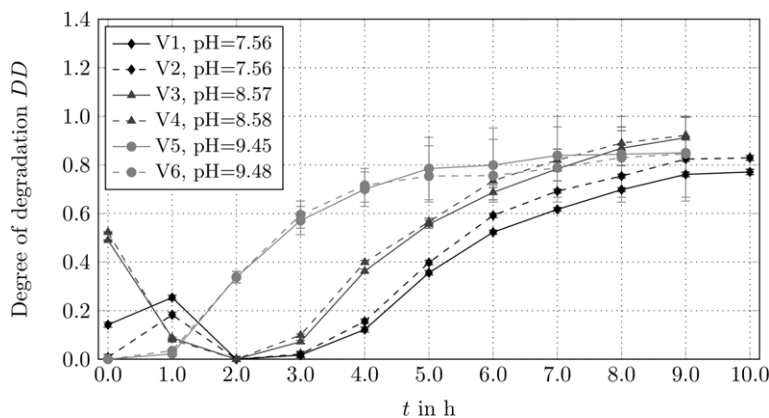


Figure 6. Degree of degradation DD of all experiments depending on the pH value.

4.2 Evaluation of the Degree of Degradation

In the following, key figures are presented that take different phenomena into account in order to evaluate the dependence of the degree of degradation on different influencing variables. The additional parameters should clarify the comparative applicability of the presented methodology and demonstrate the necessity of a constant pH value.

As a first benchmark, the half-life t_{50} is introduced, similar to the ligand half-life from McManus and Martell [2]. It represents the time after which 50 % of the original Fe-EDTA material quantity has been degraded and is defined according to Eq. (15).

$$DD(t_{50}) = 0.5 \quad (15)$$

The results of all half-lives of all experiments can be seen in Fig. 7. The diagram first suggests that the stability of Fe-EDTA decreases with increasing pH value. However, this is a fallacy, as the experimental conditions, and thus the already mentioned effects of absorption, loading, and buffering, have a significant influence on t_{50} and must therefore be considered separately.

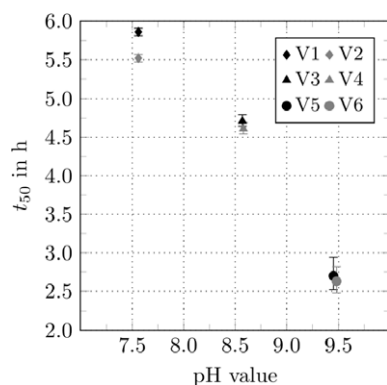


Figure 7. Half-life time t_{50} as a function of the pH.

For this reason, l_{50} is defined in Eq. (16), which compares the ratio of the $H_2S(g)$ amount of material fed in absolute to the amount of free $Fe^{2+/3+}$ that is still active. The loading l_{50} represents the absolute gaseous H_2S load that must be added to the system to cause a DD of 50 %, or until 50 % of the initial $Fe^{2+/3+}$ has precipitated.

$$l_{50} = \frac{N_{H_2S, feed}(t_{50})}{0.5N_{Fe,0}} \quad (16)$$

In this way, it is possible to compare experiments with different initial amounts of redox catalyst and different $H_2S(g)$ loads. The calculated loading l_{50} is shown in Fig. 8 and, like t_{50} , the parameter l_{50} incorrectly indicates that the stability of the redox catalyst decreases with increasing pH value. However, this conclusion is only of limited significance since the effects of increasing degradation or increased absorption efficiency are not separated from each other due to a higher pH value.

The more H_2S is reacted, the more often the redox cycle according to Eqs. (1)–(4) is run through and the more likely

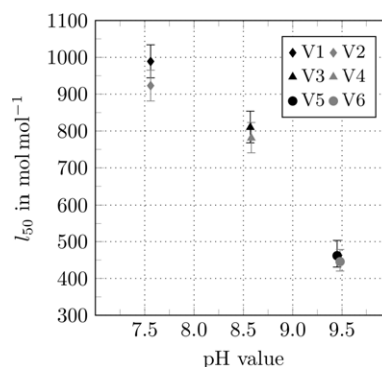


Figure 8. Gas load l_{50} in dependence on the pH value.

the degradation mechanism takes place. At a low pH value, less H_2S can be absorbed and reacts to elemental sulfur, as shown by Saelee and Bunyakan [3]. Correspondingly, the likelihood of degradation within the redox cycle is lower and the half-lives and thus l_{50} are higher. This is a consequence of the pH-dependent absorption performance, but not necessarily due to a direct influence of the pH on the Fe-EDTA.

Due to the fact that, up to now, only the gaseous H_2S load has often been considered, the absorption equilibrium is indirectly included in the stability investigation. However, this equilibrium is strongly dependent on the pH value, and if this is not kept constant, the results obtained from these studies must be viewed critically.

Therefore, it cannot be distinguished with the previous key figures whether the instability results directly from the pH value or indirectly from an increased absorption performance due to a higher pH value. Therefore, key figures must be defined that relativize the absorption under different conditions.

For this purpose, a_{50} according to Eq. (17) is defined, which sets the $H_2S(aq)$ absorbed into the liquid until t_{50} in relation to the initial active redox catalyst $Fe^{2+/3+}$.

$$a_{50} = \frac{N_{H_2S, abs}(t_{50})}{0.5N_{Fe,0}} \quad (17)$$

Fig. 9 shows the results of a_{50} and the initially assumed influence of the pH value on the stability of Fe-EDTA. This stability

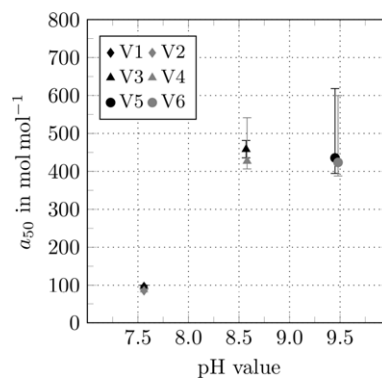


Figure 9. Consideration of the absorbed amount of $H_2S(aq)$ in relation to the initial active redox catalyst expressed by a_{50} .

increases with the pH value, which, on the one hand, is an indication of the associated strengthening of the coordinative bonds between Fe and EDTA and, on the other hand, supports the assumption of the radical mechanism according to Eqs. (5)–(8).

An increased OH^- concentration in the solution neutralizes the H^+ and H_3O^+ ions, thereby reducing the likelihood of H_2O_2 formation, which initiates the radical mechanism.

However, since the basic NH_3 solution can store and buffer the absorbed H_2S , a_{50} is not yet a fully purified key figure.

Although it considers the actual load of $\text{H}_2\text{S}(\text{aq})$, it does not consider how often the free Fe can pass through the redox cycle without degrading.

For this purpose, c_{50} is defined according to Eq. (18). This key figure relates the reactively converted H_2S until t_{50} to the initial amount of free Fe.

It indicates the number of times a $\text{Fe}^{2+/3+}$ ion can pass through the redox cycle before it precipitates with 50 % probability and is thus a benchmark for the stability analysis, which is adjusted to other pH effects.

$$c_{50} = \frac{N_{\text{H}_2\text{S, reac}}(t_{50})}{0.5N_{\text{Fe},0}} \quad (18)$$

Fig. 10 shows the results of the calculated cycle key figure and the increasing stability with increasing pH value. Furthermore, a stability maximum between pH 8 and 9 is obvious, which seems plausible.

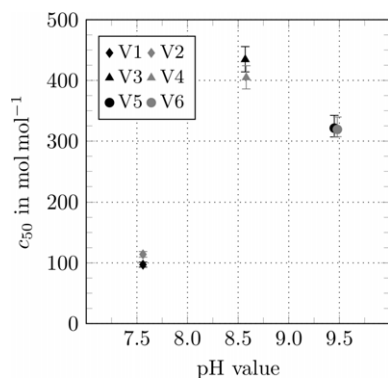


Figure 10. Circulation number c_{50} in dependence on the pH value.

The complex Fe-EDTA is formed from Fe and the weak acid EDTA, which can lead to a weakening of the coordinative bonds with decreasing pH value. In addition, the degradation mechanism is attributed to the formation and impact of hydroxyl radicals. According to McManus and Martell [2], the conditions increase with decreasing pH value, and a faster degradation is observed.

Furthermore, they write that at high pH values a good absorption performance of H_2S is achieved, but Fe can precipitate at a pH of 9 or higher as $\text{Fe}(\text{OH})_2$ or $\text{Fe}(\text{OH})_3$. This could explain the decrease of c_{50} and the appearance of the maximum pH value 8.5. In addition, the maximum lies in the usual operating range of the Fe-EDTA-based wet oxidative process

(Sulferox pH 7–8, Sulflint pH 7–9, LOCAT pH 8–8,5) [1]. The results obtained are in accordance with the pH values given in the literature [1] and show that Fe-EDTA is most stable under the given conditions at a pH value of 8.5.

5 Conclusion

The degradation tendency of different pseudo-catalysts is an important operating parameter in wet oxidative processes, because it decides on their profitability in order to keep the chemical costs within acceptable limits and to avoid high chemical make-up rates.

Furthermore, Kohl and Nielson [1] mention that, in the control of wet oxidative processes, for any given chelate, the iron chelate can exist in various forms, depending on the chelate and iron concentrations, the solution pH value, the temperature, and the overall ionic strength of the solution. “Consequently, the process conditions in the regeneration step must be such that the formation of the most stable form of ferric chelate is favored.”

The way the experiments were carried out and the key figures introduced in this work allow studying the stability on a broad basis, as various pseudo-catalysts and catalysts, feed compositions, additives, or radical scavengers can be tested. The investigations carried out show a clear pH value dependence of the Fe-EDTA stability. It was shown that, for meaningful results, the pH value must be kept constant and must be included in the evaluations of the degradation tendency.

The key figures introduced for this purpose allow the separation of different effects that are induced by the pH value, enabling an objective assessment of the degradation in the first place.

The authors have declared no conflict of interest.

Symbols used

a	[-]	absorption number
c	[-]	circulation number
DD	[-]	degree of degradation
l	[-]	gas load number
N	[mol]	molar quantity
\dot{n}	[mol s^{-1}]	molar flux
p	[bar]	pressure
R	[$\text{J mol}^{-1}\text{K}^{-1}$]	ideal gas constant (8.314)
t	[s]	time
T	[K]	temperature
\dot{V}	[L min^{-1}]	volume flow
x	[-]	mole fraction in the liquid phase
y	[-]	mole fraction in the gas phase

Greek symbols

β	[g L^{-1}]	mass concentration
ξ	[-]	mass fraction

Sub-/superscripts

0	initial conditions
50	time at which 50 % of the chelated complexes are degraded
abs	absorbed
air	air
aq	aqueous
exp	experiment
feed	feed
g	gaseous
k	discrete point in time
max	maximum
n	standard temperature and pressure (213.15 K, 1013.25 mbar)
reac	reactive
*	normalized size

Abbreviations

AIR	Analysis, Indicating, Recording (PCE category according to DIN EN 62424)
DTPA	diethylenetriaminepentaacetic acid
EDTA	ethylenedinitrilotetraacetic acid
FIR	Flow, Indicating, Recording (PCE category according to DIN EN 62424)
FIRC	Flow, Indicating, Recording, Controlling (PCE category according to DIN EN 62424)

MFC	mass flow controller
NTA	nitrilotriacetic acid
PCE	process control engineering

References

- [1] A. L. Kohl, R. Nielsen, *Gas Purification*, 5th ed., Elsevier Science, Amsterdam **1997**.
- [2] D. McManus, A. E. Martell, *J. Mol. Catal. A: Chem.* **1997**, *117* (1–3), 289–297. DOI: [https://doi.org/10.1016/S1381-1169\(96\)00254-3](https://doi.org/10.1016/S1381-1169(96)00254-3)
- [3] R. Saelee, C. Bunyakan, *ISRN Chem. Eng.* **2012**, 1–8. DOI: <https://doi.org/10.5402/2012/740429>
- [4] G. M. Deshmukh, A. Shete, *J. Anal. Bioanal. Tech.* **2012**, *3* (138), 432–436. DOI: <https://doi.org/10.4172/2155-9872.1000138>
- [5] H. J. Wubs, A. A. C. M. Beenackers, *AIChE J.* **1974**, *40* (3), 433–444. DOI: <https://doi.org/10.1002/aic.690400307>
- [6] N. Hasebe, *Chem. Econ. Eng. Rev.* **1970**, 27.
- [7] M. Avrahami, R. M. Golding, *J. Chem. Soc. A* **1968**, 647–651. DOI: <https://doi.org/10.1039/J19680000647>
- [8] J. F. Demmink, A. A. C. M. Beenackers, *Ind. Eng. Chem. Res.* **1998**, *37* (4), 1444–1453. DOI: <https://doi.org/10.1021/ie970427n>